Chinese Chemical Letters 35 (2024) 109292

Contents lists available at ScienceDirect

Chinese Chemical Letters

journal homepage: www.elsevier.com/locate/cclet

Synthesis and reactivity of cobalt dinitrogen complex supported by nonsymmetrical pincer ligand

Yuanjin Chen[a], Xianghui Shi[a], Dajiang Huang[a], Junnian Wei[a,*], Zhenfeng Xi[a,b,*]

[a] Beijing National Laboratory for Molecular Sciences (BNLMS), Key Laboratory of Bioorganic Chemistry and Molecular Engineering of Ministry of Education, College of Chemistry, Peking University, Beijing 100871, China
[b] State Key Laboratory of Organometallic Chemistry, Shanghai Institute of Organic Chemistry, Shanghai 200032, China

ARTICLE INFO

Article history:
Received 9 August 2023
Revised 29 October 2023
Accepted 9 November 2023
Available online 11 November 2023

Keywords:
Dinitrogen fixation
Dinitrogen transformation
Nonsymmetrical pincer ligand
Cobalt complex
Catalytic silylamine formation

ABSTRACT

A nonsymmetrical PNN pincer ligand [6-(^{t}Bu$_2$PNH)C$_5$H$_4$N-2-(3-Mes)C$_3$H$_2$N$_2$] and its corresponding cobalt-N_2 complex were synthesized and characterized. By the stoichiometric reaction of the PNN ligand lithium salt with $CoCl_2$, the complex **3**, (PNN)CoCl, was obtained. Then, reduction of **3** with $NaBHEt_3$ under a dinitrogen atmosphere yielded complex **5**, (PNN)Co(I)(η^1-N_2). Single-crystal X-ray analysis, IR spectrum, and DFT calculations revealed that the dinitrogen in **5** was only weakly reduced by the cobalt center. The reactions of **5** with carbon monoxide and 2,6-dimethylphenyl isocyanide gave carbonyl and isocyanide complexes **6** and **7** with the release of N_2, respectively. Furthermore, these cobalt complexes, especially complex **5**, demonstrated the capacity to convert dinitrogen to N(TMS)$_3$ with moderate efficiency.

The activation and transformation of dinitrogen gas have been one of the central focuses in the realm of chemistry. A classical approach involves the utilization of transition metal complexes. The synthesis and characterization of dinitrogen complexes offer one of the most effective strategies for understanding the diverse bonding modes of dinitrogen and its potential applications in synthesizing N-containing compounds [1–6]. Our group has developed several metal-N_2 systems and investigated their subsequent dinitrogen derivatization reactions during the past several years [7–11]. Cobalt has proven to be an important element in dinitrogen activation chemistry, with an array of cobalt dinitrogen complexes documented in the literature [12–16]. In 2021, we synthesized and structurally characterized the cobalt-bis(dinitrogen) complex [LCo(N_2)$_2$]$^-$ (L: $Cy_2PCH_2CH_2PCy_2$) with simple and commercially available bidentate phosphine ligands. Further N_2 functionalization afforded the first well-defined cobalt diazenido complex [17]. In 2022, we reported cobalt dinitrogen complexes bearing cyclopentadienyl-phosphine ligands and a phosphido-bridged binuclear cobalt complex. We also studied the reactivity of these dinitrogen complexes, providing novel insights into their potential applications in the field of dinitrogen activation and transformation [18,19].

Advancements in the design of new ligands remain pivotal for enriching our understanding of dinitrogen complexes. Pincer ligands have gained widespread usage in organometallic chemistry and organic synthesis, owing to their adaptable steric and electronic properties [20–26]. Among the diverse pincer ligands, nonsymmetrical pincer ligands and their corresponding organometallic complexes have received particular attention [27–33]. These pincer ligands offer new possibilities due to their distinct electronic structure and potential hemilability. Recently, several nonsymmetrical pincer ligand-supported metal dinitrogen complexes have been reported and begun to exhibit unique properties. For instance, Fryzuk and co-workers synthesized mononuclear cobalt dinitrogen complex using PNN ligands (phosphine-enamidoiminophosphorane) developed by their group. Although the molecular complex bears weakly bound terminal N_2, it shows extremely effective catalytic activity in the homogeneous catalytic functionalization of molecular dinitrogen to generate N(SiMe$_3$)$_3$, up to 200 TONs (*i.e.*, equivalent of N(SiMe$_3$)$_3$ formed per equivalent of catalyst) [34,35]. Meyer group used the bis(PNN) ligand (pyrazolate-based "two-in-one" pincer ligand) previously reported by their group as a research platform to successfully synthesize binuclear cobalt-dinitrogen complexes. These dinuclear cobalt complexes have been shown to mediate the silylation of N_2 to N(SiMe$_3$)$_3$, producing up to 240 equiv. of N(SiMe$_3$)$_3$ per catalyst, which is one of the highest yields to date [14,36]. Braunstein, Danopoulos, and co-workers also observed the formation of a dinitrogen-coordinated dinuclear cobalt

* Corresponding authors.
E-mail addresses: jnwei@pku.edu.cn (J. Wei), zfxi@pku.edu.cn (Z. Xi).

https://doi.org/10.1016/j.cclet.2023.109292
1001-8417/

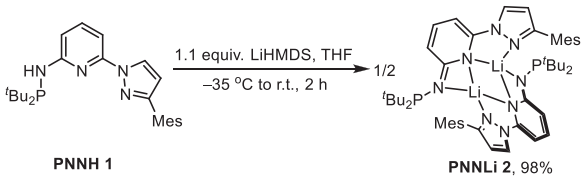

Scheme 1. Synthesis of **2**.

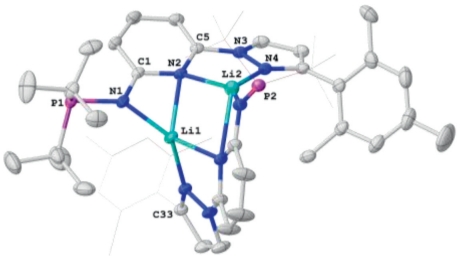

Fig. 1. The solid-state structure of **PNNLi** (**2**) with ellipsoids drawn at 30% probability. Mes group on C33 and *tert*–Butyl on P2 are shown in wireframe, and hydrogen atoms are omitted for clarity. Selected bond lengths (Å) and angles (degrees). C1–N1 1.3341(18), C1–N2 1.3882(17), C5–N2 1.3470(17), N1–Li1 1.972(3), N2–Li1 2.231(3), N2–Li2 2.257(3), N4–Li2 2.041(3), N1–Li1–N2 65.95(8), N2–Li2–N4 79.94(9).

complex in the reduction reaction of PNCCoCl under dinitrogen-depleted conditions, which otherwise are difficult to prepare [37]. Furthermore, other metal dinitrogen complexes supported by nonsymmetrical pincer ligands have also been developed [38–41]. Encouraged by these significant previous works, as well as our long-standing interest in the activation of dinitrogen by cobalt, herein, we reported a rational synthesis of a new nonsymmetrical pincer ligand. We also detail the synthesis, characterization, and reactivity of the cobalt dinitrogen complex.

The target **PNNH** [6-(^{t}Bu$_2$PNH)C$_5$H$_4$N-2-(3-Mes)C$_3$H$_2$N$_2$] (**1**) was synthesized in high yield through a three-step process starting from 2–bromo-6-fluoropyridine, as depicted in Scheme S1 (Supporting information). The methodology to synthesize the **PNNH** ligand is modular, scalable, and convenient (for details, see Supporting information). The deprotonation of **PNNH** by directly reacting **1** with 1.1 equiv. of LiHMDS in THF yielded anionic lithium salt **PNNLi** (**2**), in near quantitative yield (Scheme 1). Complex **2** was characterized by elemental analysis and ^{1}H, ^{13}C, and ^{31}P NMR spectra. The resonance in the ^{31}P NMR spectrum of **2** (69.6 ppm) is close to that (59.6 ppm) in complex **1**. Light yellow crystals **2**, suitable for X-ray diffraction studies, were obtained from hexane at room temperature. The structure of **2** indicates that the lithium atom is four-coordinate and bonded to the two nitrogen atoms of each ligand in a distorted tetrahedral geometry (Fig. 1). This result is quite different from the findings of Danopoulos and Braunstein group's research on pincer lithium and potassium complexes, where the phosphine atom participated in the interaction [42,43]. This deviation may be attributed to the stronger σ-donor capabilities of the nitrogen atoms, which make them more prone to coordinate with lithium ions.

The stoichiometric (1:1) reactions of the *in situ* generated **2** and $CoCl_2$ at −35 °C afforded the corresponding complex **3** in high yields (Scheme 2). Complex **3** exhibits a solution magnetic moment of 2.3 μ_B (measured by Evans' method in THF-d_8) at 298 K [44,45], indicative of an $S = 1/2$ ground state. Likewise, metal halides PNNCrCl and PNNFeBr can be synthesized through this method (see Supporting information for more details). Upon reaction of $CoCl_2$ with 2 equiv. of precursor, complex **4** could be obtained (Scheme 2). Magnetic susceptibility measurement at room temperature in THF-d_8 revealed a solution magnetic moment of 2.0 μ_B, consistent with a low-spin Co(II) ($S = 1/2$) complex. The vibration (3318 cm^{-1})

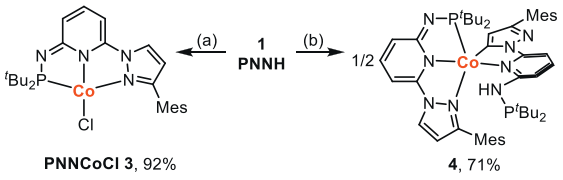

Scheme 2. Syntheses of cobalt complexes **3** and **4**. (a) 1.0 equiv. LiHMDS, THF, −35 °C to r.t., 2 h; then 1 equiv. $CoCl_2$, r.t., 12 h. (b) 1.0 equiv. LiHMDS, THF, −35 °C to r.t., 2 h; then 0.5 equiv. $CoCl_2$, r.t., 12 h.

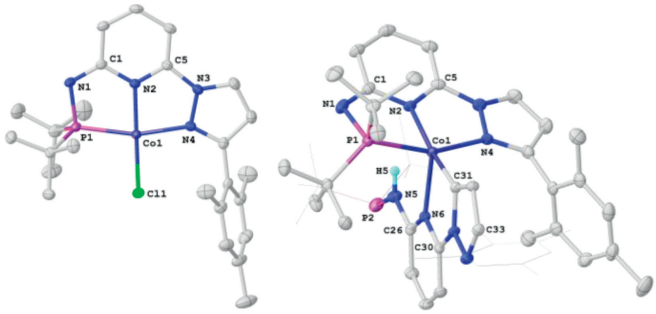

Fig. 2. The solid-state structures of **3** (left) and **4** (right) with ellipsoids drawn at 30% probability. Mes group on C33 and *tert*–Butyl on P2 are shown in wireframe, and hydrogen atoms attached to carbon are omitted for clarity. Selected bond lengths (Å) and angles (degrees). **3**: C1–N1 1.317(2), C1–N2 1.390(2), P1–N1 1.6763(13), Co1–P1 2.1952(4), Co1–N4 1.9957(13), Co1–N2 1.8856(12), Co1–Cl1 2.1854(4), P1-Co1-Cl1 98.129(16), N4-Co1-Cl1 98.16(4). **4**: C1–N1 1.322(4), C1–N2 1.393(4), C5–N2 1.340(4), P1–N1 1.681(3), Co1–P1 2.2295(9), Co1–N2 1.948(2), Co1–N4 2.046(3), C26–N5 1.381(4), C26–N6 1.355(4), C30–N6 1.354(4), P2–N5 1.734(3), Co1–C31 1.910(3), N2–Co1–P1 80.90(8), N2–Co1–N4 80.27(10), N6–Co1–C31 80.69(11).

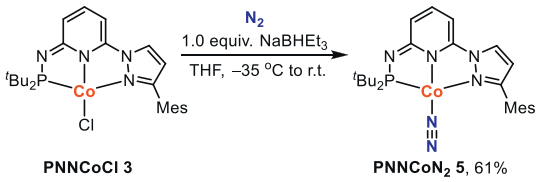

Scheme 3. Synthesis of **5**.

of **4** in the IR spectrum indicates the presence of a N–H bond (Fig. S37 in Supporting information). Red crystals of **4** suitable for X-ray diffraction studies were obtained from the mixture of tetrahydrofuran and *n*-hexane at room temperature. The structural analysis of **4** shown in Fig. 2 exhibits bond distances of 1.322(4) (C1–N1), 1.393(4) (C1–N2), 1.340(4) (C5–N2), as well as 1.381(4) (C26–N5), 1.355(4) (C26–N6), 1.354(4) (C30–N6) Å, respectively, further suggesting an unexpected hydrogen atom migration. This may be due to the high steric hindrance of this ligand, which prevents the simultaneous coordination of two ligands.

The reaction of complex **3** with $NaHBEt_3$ was then explored (Scheme 3). Treatment of **3** with one equivalent of $NaHBEt_3$ at −35 °C under N_2 led to a purple solution, from which the Co(I)–N_2 complex **5** was obtained in 61% isolated yield after work-up. The molecular structure of **5** was characterized by single-crystal X-ray structural analysis (Fig. 3).

The sum of the internal angles around the cobalt atom revealed a virtually planar geometry, amounting to 358.03°. The N5–N6 distance of 1.0903(19) Å is comparable to that of free N_2 (1.098 Å). The Co1–N2 distance of 1.8863(12) Å is slightly shorter than those found in the Co(I) mononuclear dinitrogen complexes reported by Chirik (1.9439(12) Å) [46] and Danopoulos (1.904(2) Å) [37]. Similarly, the bond lengths of Co1–P1 show the same trend and are slightly shorter than those disclosed by Chirik [46] and Danopoulos [37]. In addition, the N–N vibration (2056 cm^{-1}) of **5** is similar to

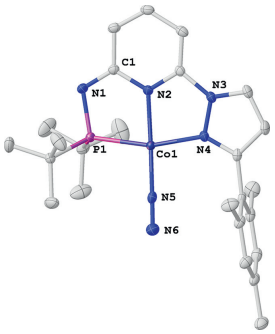

Fig. 3. The solid-state structure of **5** with ellipsoids drawn at 30% probability. Hydrogen atoms are omitted for clarity. Selected bond lengths (Å) and angles (degrees). C1–N1 1.3192(19), C1–N2 1.3896(18), Co1–P1 2.1809(4), Co1–N2 1.8863(12), Co1–N4 1.9483(12), Co1–N5 1.7713(13), N5–N6 1.0903(19), P1–Co1–N5 97.64(4), N4–Co1–N5 99.07(5), N2–Co1–P1 81.70(4), N2–Co1–N4 81.62(5).

those of other non-symmetric pincer ligand Co(I) complexes with end-on bound N_2 (within the range of 1973 to 2071 cm^{-1}) [34–37], reflecting a weak activation of N_2 [47]. The $^{15}N_2$-labeled sample of **5**, prepared under $^{15}N_2$ atmosphere at room temperature, showed $^{15}N–^{15}N$ stretching vibration at 1988 cm^{-1} (Fig. S41 in Supporting information). As an extension of this work, we also obtain the dinitrogen complexes of the heavier group 9 metals (Rh and Ir). Interestingly, comparing the N–N bond distances of the group 9 metals (Co, Rh and Ir) dinitrogen complexes supported by PNN ligand, the largest bond length difference is only 0.06 Å (Table S11 in Supporting information).

To further understand the electronic structure of complex **5**, density functional theory (DFT) calculations have been performed. The computation methodology is detailed in Supporting information. The optimized structure in the gas phase agrees with the crystal data (Fig. S8 in Supporting information). The calculated Co–N(Py) and N–N bond lengths of 1.895 and 1.117 Å are close to the experimentally determined values of 1.8863(12) and 1.0903(19) Å, indicating that the level of theory used here is reliable. Fuzzy atom bond order (FBO) suggested by Mayer and Salvador [48] agrees well with the classical chemical notions and exhibits small basis sensitivity. The FBOs of the N5–N6 bond in **5** is 2.66, while that of Co–N5 is 1.32. These results indicate that N_2 is indeed only weakly reduced by the cobalt center. The HOMO (Highest Occupied Molecular Orbital), HOMO-1, and LUMO (Lowest Unoccupied Molecular Orbital) are depicted in Fig. 4. Orbital composition analysis of complex **5** was also carried out (Hirshfeld method). The HOMO predominantly consists of the d-orbital of the Co atom, with the cobalt center contributing 90.4% while the two N atoms contribute only 1.5%. In contrast, the LUMO is primarily located on the pincer ligand, with the cobalt center contributing only 6.6% while the two N atoms make up 7.6%. In the HOMO-1 orbital, cobalt and dinitrogen exhibit a higher contribution, with the feedback bonding character of the dinitrogen.

The reductive behaviors of complex **5** with many reductants were investigated. Unfortunately, no pure reduced species have been isolated to date. However, treating **5** with carbon monoxide (CO) and 1 equiv. of 2,6-dimethylphenyl isocyanide (XylNC) yielded the monomeric cobalt carbonyl (**6**) and cobalt isocyanide (**7**), respectively (Scheme 4). The resonances in the ^{31}P NMR spectra of **6** (150.4 ppm) and **7** (148.3 ppm) slightly shift to low-field, compared with that (139.1 ppm) in the dinitrogen complex **5**. Single crystals of **6** and **7**, suitable for X-ray diffraction analysis, were obtained from *n*-hexane at −35 °C (Fig. 5). In the structures of **6** and **7**, the Co1–N2 distances of 1.9036(11) and 1.9038(13) Å are slightly longer than those determined in the cobalt halides **3** [1.8856(12) Å] and dinitrogen complex **5** [1.8863(12) Å].

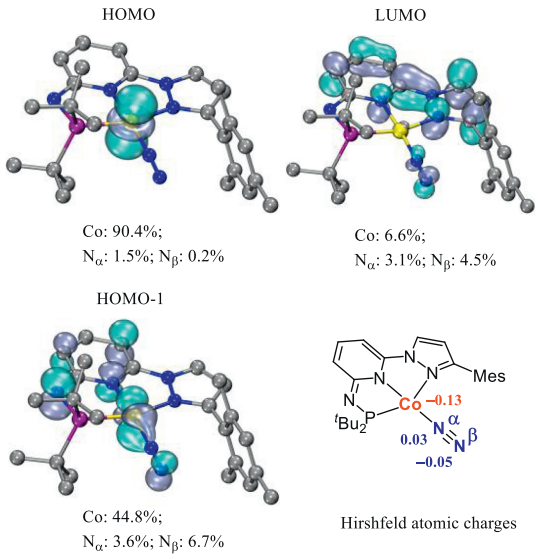

Fig. 4. The HOMO, LUMO, and HOMO-1 orbitals (isovalue = 0.05) and Hirshfeld atomic charges of **5**.

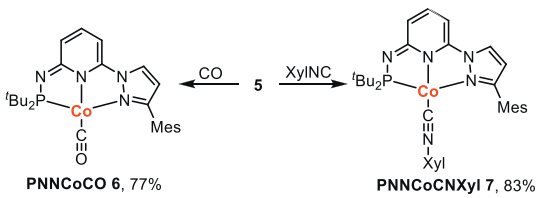

Scheme 4. Syntheses of **6** and **7** (Xyl = 2,6-dimethylphenyl).

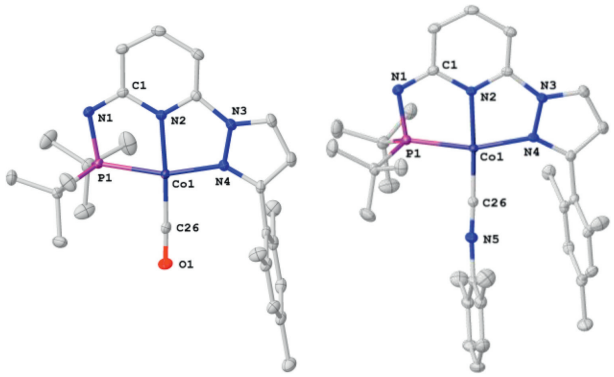

Fig. 5. The solid-state structures of **6** (left) and **7** (right) with ellipsoids drawn at 30% probability. Hydrogen atoms are omitted for clarity. Selected bond lengths (Å) and angles (degrees). **6**: C1–N1 1.3187(17), C1–N2 1.3873(16), Co1–P1 2.1723(4), Co1–N2 1.9036(11), Co1–N4 1.9361(11), Co1–C26 1.7149(14), C26–O1 1.1578(17), C26-Co1-P1 95.45(5), C26-Co1-N4 101.82(6); **7**: C1–N1 1.315(2), C1–N2 1.390(2), Co1–P1 2.1602(4), Co1–N2 1.9038(13), Co1–N4 1.9454(13), Co1–C26 1.7518(16), C26–N5 1.181(2), C26–Co1–P1 95.66(5), C26–Co1–N4 101.74(6).

We then investigated the catalytic formation of silylamine from dinitrogen using **5** as a catalyst. The study involved screening reducing agents, solvents, and reaction times to determine optimal reaction conditions. It was found that the most favorable condition for the reaction was achieved using 2000 equiv. of potassium (relative to **5**), dissolved in THF, at room temperature and atmospheric pressure for 48 h. The optimized condition resulted in 33.4 equiv. of $N(TMS)_3$ (Table 1, entry 7). In addition, we explored the catalytic activity of other metal halides supported by our nonsymmetrical PNN ligand as alternative catalysts. The yields of $N(TMS)_3$ were 31.5, 14.2, and 8.1 equiv., respectively (Table 1, entries 9, 10, and 11).

Table 1
Catalytic formation of $N(SiMe_3)_3$ from N_2 by PNN-metal complex as catalyst.[a]

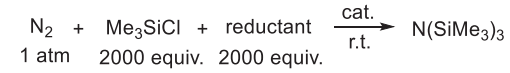

Entry	Cat.	Red.	Time (h)	Equiv. based on cat.
1[b]	$PNNCoN_2$	KC_8	16	9.2
2[b]	$PNNCoN_2$	K	16	5.6
3	$PNNCoN_2$	KC_8	16	17
4	$PNNCoN_2$	K	24	18.5
5	$PNNCoN_2$	K	36	29.8
6	$PNNCoN_2$	K	48	30.7
7	$PNNCoN_2$	K	72	33.4
8	$PNNCoN_2$	K	48	33.4
9	PNNCoCl	K	48	31.5
10	PNNCrCl	K	48	14.2
11	PNNFeBr	K	48	8.1

[a] Condition: a mixture of catalyst (0.005 mmol), reductant (10.0 mmol, 2000 equiv.), and Me_3SiCl (10.0 mmol, 2000 equiv.) was stirred in THF at room temperature for 48 h under 1 atm dinitrogen. The averages of multiple runs are shown.
[b] Et_2O is used as the solvent.

To probe the reaction mechanism, we carried out *in situ* reduction experiments on complex **5**. Within a dinitrogen-filled glovebox, 10 equiv. of potassium were added into a THF solution of complex **5** at room temperature. After 0.5 h, the coordinated dinitrogen peak at 2056 cm^{-1} vanished, and two new peaks appeared at 1777 cm^{-1} and 1957 cm^{-1} (Fig. S1 in Supporting information). After 1 h, the infrared spectrum remained unchanged from that at 0.5 h. Subsequently, we introduced 3 equiv. of TMSCl to the mixture. After 15 min, both the 1777 cm^{-1} peak and 1957 cm^{-1} peak disappeared, and we re-observed the dinitrogen peak of complex **5** at 2057 cm^{-1}. Concurrently, it is worth noting that in this catalytic synthesis of $N(TMS)_3$, $Me_3SiSiMe_3$ was detected as a byproduct (confirmed by GC, see Supporting information). This byproduct is likely due to $Me_3Si\cdot$ recombination. Under the reductive conditions, TMSCl can generate silyl radicals, a phenomenon being documented in the literature [49].

Further, we carried out DFT calculations to preliminarily explore the mechanism (Fig. S16 in Supporting information). The computational results predicted an N≡N infrared vibrational peak for complex **5** at 2183 cm^{-1}. Meanwhile, the reduced anionic form of complex **5** ($PNNCoN_2^-$) was predicted to exhibit a vibrational peak at 1982 cm^{-1}. Comparing these predictions with our experimental observations suggested that the initial reduction step might transform complex **5** into its anionic form. However, other unknown products might also be formed. The calculated energies indicated that the sequential addition of two trimethylsilyl radicals to the distal nitrogen atom, leading to the formation of [PNNCoNN($SiMe_3$)x)] complexes ($x = 1$ and 2) was possible. Corresponding free energy changes (ΔG_{298}) were −12.5 kcal/mol (I, $x = 1$) and −21.6 kcal/mol (II, $x = 2$) at 298 K, respectively. It is still challenging to provide comprehensive mechanistic speculation due to limited experimental evidence. Cobalt-catalyzed dinitrogen silylation likely proceeds *via* a silyl-radical-based pathway. However, we cannot rule out a pathway that involves the stepwise reduction and electrophilic silylation of coordinated dinitrogen.

In conclusion, we synthesized and characterized a novel PNNH ligand, the corresponding lithium complex, and the Co(I) dinitrogen complex. The Co(I) dinitrogen complex easily undergoes substitution reaction with carbon monoxide and 2,6-dimethylphenyl isocyanide to generate carbonyl and isocyanide complexes along with the release of dinitrogen. We further showed the capability of these complexes, supported by the nonsymmetrical pincer ligand, to act as catalysts for the conversion of dinitrogen into $N(TMS)_3$. We believe that our study can serve as a springboard for future research and hold potential for valuable contributions to the development of future catalysts.

Declaration of competing interests

The authors declare that they have no known competing financial interests or personal relationships that could have appeared to influence the work reported in this paper.

Acknowledgments

This work was supported by the National Natural Science Foundation of China (Nos. 21988101 and 22201013) and Beijing Natural Science Foundation (No. 2222008). The DFT calculation was supported by the High-performance Computing Platform of Peking University. The authors thank the NMR facility of National Center for Protein Sciences at Peking University.

Supplementary materials

Supplementary material associated with this article can be found, in the online version, at doi:10.1016/j.cclet.2023.109292.

References

[1] D. Singh, W.R. Buratto, J.F. Torres, L.J. Murray, Chem. Rev. 120 (2020) 5517–5581.
[2] Z.J. Lv, J. Wei, W.X. Zhang, et al., Natl. Sci. Rev. 7 (2020) 1564–1583.
[3] S. Kim, F. Loose, P.J. Chirik, Chem. Rev. 120 (2020) 5637–5681.
[4] R.J. Burford, M.D. Fryzuk, Nat. Rev. Chem. 1 (2017) 0026.
[5] I. Čorić, P.L. Holland, J. Am. Chem. Soc. 138 (2016) 7200–7211.
[6] J. Zeng, J. Su, F. You, J. Zhu, Chin. Chem. Lett. 34 (2023) 107759.
[7] Z.B. Yin, B. Wu, G.X. Wang, J. Wei, Z. Xi, J. Am. Chem. Soc. 145 (2023) 7065–7070.
[8] G.X. Wang, X. Wang, Y. Jiang, et al., J. Am. Chem. Soc. 145 (2023) 9746–9754.
[9] G.X. Wang, J. Yin, J. Li, et al., CCS Chem. 3 (2021) 308–316.
[10] J. Yin, J. Li, G.X. Wang, et al., J. Am. Chem. Soc. 141 (2019) 4241–4247.
[11] Z.J. Lv, Z. Huang, W.X. Zhang, Z. Xi, J. Am. Chem. Soc. 141 (2019) 8773–8777.
[12] C.C. Lu, S.D. Prinslow, Group 9 transition metal–dinitrogen complexes, in: Y. Nishibayashi (Ed.), Transition Metal-Dinitrogen Complexes: Preparation and Reactivity, Wiley-VCH, Weinheim, 2019, pp. 337–402.
[13] Y. Dong, P. Zhang, Q. Fan, et al., Inorg. Chem. 59 (2020) 16489–16499.
[14] S. Kuriyama, S. Wei, H. Tanaka, et al., Inorg. Chem. 61 (2022) 5190–5195.
[15] Y. Zhang, X. Pan, M. Xu, et al., Inorg. Chem. 62 (2023) 3836–3846.
[16] L. Gu, A. Fraker, A. McSkimming, Organometallics. 42 (2023) 1621–1628.
[17] M. Zhong, X. Cui, B. Wu, et al., CCS Chem. 4 (2022) 532–539.
[18] H.J. Li, R. Feng, G.X. Wang, J. Wei, Z. Xi, Dalton Trans. 51 (2022) 16811–16815.
[19] G.X. Wang, X. Yan, J. Yin, et al., Chem. Eur. J. 28 (2022) e2022028.
[20] K.J. Szabo, O.F. Wendt, Pincer and Pincer-Type Complexes: Applications in Organic Synthesis and Catalysis, Wiley-VCH, Weinheim, 2014.
[21] M. Asay, D. Morales-Morales, Dalton Trans. 44 (2015) 17432–17447.
[22] M. Asay, D. Morales-Morales, Top. Organomet. Chem. 54 (2015) 239–268.
[23] G. van Koten, R.A. Gossage, M. Albrecht, The Privileged Pincer-Metal Platform: Coordination Chemistry & Applications, Topics in Organometallic Chemistry, Springer, Cham, 2016.
[24] S. Murugesan, K. Kirchner, Dalton Trans. 45 (2016) 416–439.
[25] D. Morales-Morales, Pincer Compounds: Chemistry and Applications, Elsevier, Amsterdam, 2018.
[26] H. Valdés, M.A. Gar-cía-Eleno, D. Canseco-Gonzalez, D. Morales-Morales, ChemCatChem. 10 (2018) 3136–3172.
[27] M. Asay, D. Morales-Morales, Dalton Trans. 44 (2015) 17432–17447.
[28] Y. Wang, Z. Huang, G. Liu, Z. Huang, Acc. Chem. Res. 55 (2022) 2148–2161.
[29] P. Sanchez, M.E. Hernandez-Juarez, E. Alvarez, et al., Dalton Trans. 45 (2016) 16997–17009.
[30] A.V. Polezhaev, C.H. Chen, Y. Losovyj, K.G. Caulton, Chem. Eur. J. 23 (2017) 8039–8050.
[31] D. Himmelbauer, H. Schratzberger, M.G. Käfer, et al., Organometallics 40 (2021) 3331–3340.
[32] Z. Huang, S. Wang, X. Zhu, et al., Chin. J. Chem. 39 (2021) 3360–3368.
[33] D. Hong, T. Rajeshkumar, S. Zhu, et al., Sci. China Chem. 66 (2023) 117–126.
[34] T. Suzuki, K. Fujimoto, Y. Takemoto, et al., ACS Catal. 8 (2018) 3011–3015.
[35] C.A. Sanz, C.A.M. Stein, M.D. Fryzuk, Eur. J. Inorg. Chem. 2020 (2020) 1465–1471.
[36] M. Li, S.K. Gupta, S. Dechert, S. Demeshko, F. Meyer, Angew. Chem. Int. Ed. 60 (2021) 14480–14487.
[37] T. Simler, P. Braunstein, A.A. Danopoulos, Chem. Commun. 52 (2016) 2717–2720.
[38] C. Hu, Y. Ding, Y. Bai, L. Guo, C. Cui, Chem. Commun. 58 (2022) 13795–13798.
[39] N.I. Regenauer, H. Wadepohl, D.A. Roşca, Inorg. Chem. 61 (2022) 7426–7435.

[40] N.I. Regenauer, H. Wadepohl, D.A. Roşca, Chem. Eur. J. 28 (2022) e2022021.
[41] M. Feller, Y. Diskin-Posner, L.J.W. Shimon, E. Ben-Ari, D. Milstein, Organometallics 31 (2012) 4083–4101.
[42] T. Simler, A.A. Danopoulos, P. Braunstein, Chem. Commun. 51 (2015) 10699–10702.
[43] T. Simler, L. Karmazin, C. Bailly, P. Braunstein, A.A. Danopoulos, Organometallics 35 (2016) 903–912.
[44] D.F. Evans, J. Chem. Soc. (1959) 2003–2005.
[45] S.K. Sur, J. Magn. Reson. 82 (1989) 169–173.
[46] S.P. Semproni, C. Milsmann, P.J. Chirik, J. Am. Chem. Soc. 136 (2014) 9211–9224.
[47] B.P. Stoicheff, Can. J. Phys. 32 (1954) 630–634.
[48] I. Mayer, P. Salvador, Chem. Phys. Lett. 383 (2004) 368–375.
[49] D.R. Weyenberg, L.H. Toporcer, A.E. Bey, J. Org. Chem. 30 (1965) 4096–4101.